A General Mechanistic Scheme for Intramolecular Electrochemical Hydrocyclizations. Mechanism of the Electroreductive Cyclization of ω-Keto-α,β-unsaturated Esters

Albert J. Fry,*,† R. Daniel Little,*,‡ and Joseph Leonetti‡

Department of Chemistry, Wesleyan University, Middletown, Connecticut 06459, and Department of Chemistry, University of California, Santa Barbara, California 93106

Received March 15, 1994®

A systematic procedure is suggested for formulating possible mechanisms by which electrochemical hydrocyclization and dehydrocyclization can occur. A combination of linear sweep voltammetry (LSV) and chemical and electrochemical arguments can be used to reduce the mechanistic possibilities to a small set or even a unique mechanism. The procedure is applied to the reductive cyclization of ω-keto-α,β-unsaturated esters. Of the several hundred mechanistic possibilities for this process, the combination of LSV and chemical arguments can reduce the list to four; preparative-scale electrolysis of a specially designed substrate permits assignment of a unique mechanism, the e–P–d–c–p path, at low concentrations of electroactive substance.

Electrochemical hydrocyclizations are processes in which electrochemical reduction of a substance consisting of two functional groups, A and B, connected by a tether results in ring formation and uptake of hydrogen. Conversely, a dehydrocyclization is a process in which *loss* of hydrogen is concomitant with ring formation (Figure 1). Many such processes are known (Scheme 1).[1] Since direct transfer of two electrons or two protons in a single step is kinetically improbable, most such cyclizations involve five consecutive steps (addition or loss of the four elementary particles plus the cyclization step itself).[2] The primary mechanistic problem posed by such processes is determination of the order in which the five chemical steps take place and, of these, which is rate-determining. Linear sweep voltammetry (LSV) provides a powerful method for analyzing such problems.[3] The LSV method involves measurement of the voltammogram of the electroactive substance of interest under a wide range of conditions. The dependence of the voltammetric peak potential (E_p) upon experimental parameters is measured under conditions where the rates of the coupled chemical reactions are fast compared to the potential scan rate.[4] The dependence of E_p upon each of several variables is measured; these include (a) the potential scan rate (v); (b) the concentration of the electroactive substance, and (c) the concentration of a second component of the solution which is known to react with an intermediate

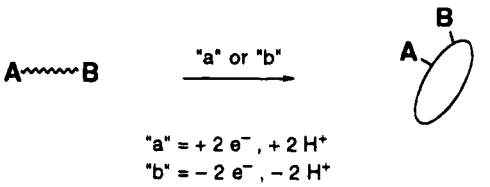

Figure 1. (a) Hydrocyclization. (b) Dehydrocyclization.

in the electrode process (for hydrocyclizations, this component would be a proton donor).[5] The observed responses are compared with those expected theoretically for various mechanisms postulated for the process under scrutiny. Frequently, such experiments permit the list of postulated mechanisms to be reduced to a much smaller list or sometimes even a unique mechanism.

Although this is a powerful method for mechanistic analysis, it rests on the key assumption that the actual mechanism is one of the mechanisms originally postulated for the electrode process. In view of the large number of mechanisms which are possible for a given reaction (*vide infra*), dependence upon the accuracy of one's intuition in this matter is unsatisfactory. It would be much more appealing to have available a list of *all* possible mechanisms. Confident from the outset that the true mechanism is included in the list, one could then proceed to reduce it to one or more reasonable alternatives by a combination of electrochemical experiment and chemical argument. We propose here a method for constructing such a complete list and apply the procedure to elucidation of the mechanism of a previously reported[6] hydrocyclization reaction.

Our discussion will be couched in terms of reductive processes, but the ideas may be applied in straightforward fashion to oxidative cyclizations. We will use the terminology of Savéant[5] to describe each mechanistic possibility (Table 1). In this formalism, each step is denoted by a lower case letter except for the rate determining step, which is represented by a capital letter. The distinction between the symbols "e" and "d" for the second electron transfer step lies in the source of the

† Wesleyan University.
‡ University of California, Santa Barbara.
® Abstract published in *Advance ACS Abstracts,* August 1, 1994.

(1) (a) Ronlan, A.; Hammerich, O.; Parker, V. D. *J. Am. Chem. Soc.* **1973**, *95*, 7132. (b) Aalstad, B.; Parker, V. D. *Acta Chem. Scand.* **1982**, *36B*, 187. (c) Shono, T.; Kise, N.; Shirakawa, E.; Matsumoto, H.; Okazaki, E. *J. Org. Chem.* **1991**, *56*, 3063. (d) Reynolds, R.; Line, L.; Nelson, R. F. *J. Am. Chem. Soc.* **1974**, *96*, 1087. (e) Mandell, L.; Daley, R. F.; Day, R. A., Jr. *J. Org. Chem.* **1976**, *41*, 4087.

(2) More complex electrocyclization sequences have been found, e.g., those involving (a) disproportionation of an initial radical ion (Aalstad, B.; Parker, V. D. *Acta Chem. Scand.* **1982**, *36B*, 187) or (b) its complexation with water or solvent (Parker, V. D. *Acta Chem. Scand.* **1981**, *35B*, 279).

(3) For example: (a) Nadjo, L.; Savéant, J. M. *J. Electroanal. Chem.* **1973**, *48*, 113; (b) Andrieux, C. P.; Savéant, J. M. *J. Electroanal. Chem.* **1974**, *53*, 165.

(4) Strictly speaking, the rates of the coupled chemical processes must exceed the polarization rate, which is related to the relative rates of diffusion, heterogeneous electron transfer, and scan rate. LSV cannot provide useful information if the coupled chemical reactions are so fast that a Nernstian equilibrium cannot be maintained on the voltammetry time scale, that is, if the initial charge transfer step is rate-limiting.

(5) Andrieux, C. P.; Savéant, J. M. *J. Electroanal. Chem.* **1974**, *53*, 165.

(6) R. L.; Moëns; Baizer, M. M. *J. Org. Chem.* **1988**, *53*, 2287.

0022-3263/94/1959-5017$04.50/0

Scheme 1

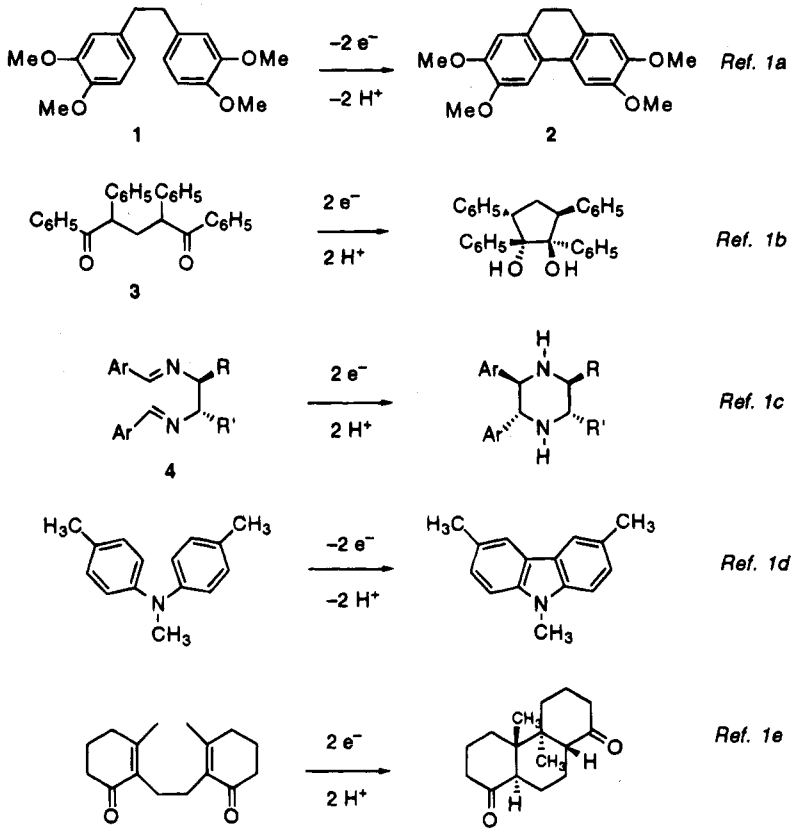

Table 1. Symbols Used To Describe Individual Steps in Electrocyclization Mechanisms

e	charge (heterogeneous) electron transfer at the electrode
d	homogeneous electron transfer (see the text)
c	cyclization (assumed to occur in homogeneous solution)
p	homogeneous protonation reaction, pseudo-first-order in proton donor

electron. If the electrode supplies the electron, the step is an "e" (heterogeneous) step; if the electron is donated in homogeneous solution by an earlier intermediate in the reaction sequence, the step is a "d" (disproportionation) step.[7,8]

The symbol "p" stands for addition or loss of a proton, depending on whether one is dealing with hydrocyclization or dehydrocyclization. Since a reductive cyclization requires two electron and two proton transfer steps in addition to the cyclization step itself, we may describe any particular mechanism by a combination of five letters, one of which is capitalized to represent the rate-determining step.[9] Parker has shown, for example, that the oxidative electrochemical cyclization of 1,2-bis(3,4-dimethoxyphenyl)ethane (**1**) to the dihydrophenanthrene **2** (which undergoes subsequent *in situ* oxidation to the corresponding phenanthrene)[10] and the reductive cyclization of 1,3-dibenzoyl-1,3-diphenylpropane (**3**) to the corresponding pinacol[1b] both proceed by the e–c–D–p–p path. The mechanism may even depend on experimental conditions: 3,4,3′-trimethoxybibenzyl (**5**) undergoes anodic cyclization by attack of the radical cation of the more highly substituted ring upon the other neutral ring at low anode potentials and by coupling of two radical cations at high anode potentials.[11]

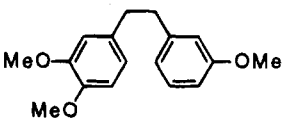

5

The number of possible permutations of two heterogeneous electron transfers, two proton transfers, and a cyclization step is given by 5!/2!2! (≡30). While the first electron transfer must necessarily be heterogeneous, the second may be either heterogeneous or homogeneous. Therefore each of these 30 paths has a counterpart in which the second step is of "d" type. The 60 permutations are presented in Table 2. Columns 1 and 2 contain all the mechanisms in which the first step is an "e" step; columns 3 and 4 contain all mechanisms in which the first step is "p" (protonation), and columns 5 and 6 contain all mechanisms in which the first step is "c" (cyclization). For the mechanisms in columns 1, 3, and 5, the second electron transfer step is heterogeneous, whereas this step is homogeneous for those in columns 2, 4, and 6. It should be noted at this point that experience has shown that in almost all cases the second electron transfer is of homogeneous ("d") type.[12] Since any of the five steps in each of the mechanisms of Table 2 might be rate-determining, Table 2 implies the exist-

(7) *J. Electroanal. Chem.* **1973**, *42*, 223.
(8) Although it may not be immediately obvious that the second electron transfer is a disproportionation, this follows from the fact that the two species involved in the electron exchange are at the same oxidation level. See Evans, D. H. *Chem. Rev.* **1990**, *90*, 743.
(9) It is possible to find systems which are not handled well by this terminology, e.g., situations in which two reactions in the sequence have comparable rate constants so that neither is rate determining.
(10) Aalstad, B.; Ronlán, A.; Parker, V. D. *Acta Chem. Scand.* **1982**, *36B*, 171.
(11) Parker, V. D.; Ronlán, A. *J. Am. Chem. Soc.* **1975**, *97*, 4714.
(12) Amatore, C. M.; Savéant, J. M. *J. Electroanal. Chem.* **1978**, *86*, 227.

Table 2. Possible Mechanistic Paths for Reductive Cyclization[a]

mechanisms initiated by heterogeneous electron transfer				mechanisms initiated by protonation				mechanisms initiated by cyclization			
1	e-e-c-p-p	13	e-d-c-p-p	25	p-c-e-e-p	37	p-c-e-d-p	49	c-e-e-p-p	55	c-e-d-p-p
2	e-e-p-c-p	14	e-d-p-c-p	26	p-c-e-p-e	38	p-c-e-p-d	50	c-e-p-p-e	56	c-e-p-p-d
3	e-e-p-p-c	15	e-d-p-p-c	27	p-c-p-e-e	39	p-c-p-e-d	51	c-e-p-e-p	57	c-e-p-d-p
4	e-c-e-p-p	16	e-c-d-p-p	28	p-e-c-e-p	40	p-e-c-d-p	52	c-p-e-p-e	58	c-p-e-p-d
5	e-c-p-e-p	17	e-c-p-d-p	29	p-e-c-p-e	41	p-e-c-p-d	53	c-p-e-e-p	59	c-p-e-d-p
6	e-c-p-p-e	18	e-c-p-p-d	30	p-e-p-c-e	42	p-e-p-c-d	54	c-p-p-e-e	60	c-p-p-e-d
7	e-p-c-e-p	19	e-p-c-d-p	31	p-e-p-e-c	43	p-e-p-d-c				
8	e-p-c-p-e	20	e-p-c-p-d	32	p-e-e-c-p	44	p-e-d-c-p				
9	e-p-p-c-e	21	e-p-p-c-d	33	p-e-e-p-c	45	p-e-d-p-c				
10	e-p-e-c-p	22	e-p-d-c-p	34	p-p-e-e-c	46	p-p-e-d-c				
11	e-p-e-p-c	23	e-p-d-p-c	35	p-p-e-c-e	47	p-p-e-c-d				
12	e-p-p-e-c	24	e-p-p-d-c	36	p-p-c-e-e	48	p-p-c-e-d				

[a] Symbols as defined in the text.

Table 3. Mechanistic Variations and Voltammetric Criteria for Representative Electrocyclization Sequences

	Mechanism	a^a (mV/decade)	b^b (mV/decade)	c^c (mV/decade)
5b	e-C-p-e-p	−29.6	0	0
5c	e-c-P-e-p	−29.6	0	29.6
5d	e-c-p-E-p	−14.8	0	14.8
17b	e-C-p-d-p	−29.6	0	0
17c	e-c-P-d-p	−29.6	0	29.6
17d	e-c-p-D-p	−19.7	0	19.7
10b	e-P-e-c-p	−29.6	0	29.6
10c	e-p-E-c-p	−14.8	0	14.8
10d	e-p-e-C-p	−14.8	0	14.8
22b	e-P-d-c-p	−29.6	0	29.6
22c	e-p-D-c-p	−19.7	0	19.7
22d	e-p-d-C-p	−19.7	0	19.7

[a] $\partial E_p/\partial(\log v)$. [b] $\partial E_p/\partial(\log[A])$. [c] $\partial E_p/\partial(\log[HX])$. Values calculated at 25 °C.

ence of 300 discrete hydrocyclization mechanisms.[13] Table 3, for example, shows some representative mechanisms which are possible in the 5−17 and 10−22 mechanistic manifolds. Finally, it must be recognized that when A ≠ B, two equivalent families of mechanism must be recognized, one derived by reduction of functional group A and the other by reduction of B. In general, therefore, when A ≠ B there are actually 600 distinct paths by which the cyclizations of Figure 1 may take place.[2] We advocate beginning any mechanistic analysis by considering all of these as possible *a priori* and then using a combination of chemical argument and electrochemical experiment to reduce the list of possibilities as much as possible.

In any particular case, it will be possible to exclude many of the mechanisms shown in Table 2 at the outset by considering the chemical nature of the system in question. For example, most reductive cyclizations of neutral substrates are initiated by transfer of an electron from the electrode to the organic substrate; hence, most mechanisms will be found among those listed in columns 1 and 2 of Table 2. However, examples of electrocyclizations proceeding by initial protonation (Table 2, columns 3 and 4) are easily found among basic substrates; e.g., bis-imine **4** is reduced as its conjugate acid (whether it is mono- or diprotonated is not clear) in acidic media,[1c] and it is even possible to conceive of hydrocyclization processes in which the first step is the cyclization step itself (*vide infra*).

A mechanistic study by LSV consists of measurement of the LSV peak potential (E_p) over a wide range of scan rates (v) and concentrations of the electroactive substance and proton donor. When the rate of the overall electrode process is limited by that of a single step in the sequence, plots of E_p vs the logarithm of (1) the potential scan rate v, (2) the concentration of the electroactive substance, and (3) the concentration of added proton donor are linear with slopes corresponding to (fractional) multiples of $RT/n\mathcal{F}$, where $\mathcal{F}$ is the symbol for the Faraday constant. We may designate the slopes of these lines as a, b, and c, respectively.[14] Conventional practice dictates that the theoretical values of a, b, and c be determined for each mechanism under consideration by carrying out a large number of digital computer simulations.[3] Simulation of all 300 mechanistic schemes implied by Table 2 (the large majority of which have not been treated previously in the literature) would be a formidable task. However, Parker has proposed[15] a set of empirical generalizations (Table 4) which can be used in the absence of simulations to predict the dependence of the LSV peak potential on changes in experimental parameters. The rules predict,

Table 4. Empirical Rules for Estimating LSV Peak Potential Behavior for Electrohydrocyclizations[a]

number and type of electron transfer steps before and during RDS	$-\partial E_p/\partial(\log v)^a$ (mV/decade)[b]	number and type of electron transfer steps before and during RDS	$-\partial E_p/\partial(\log v)^a$ (mV/decade)[b]
e	29.6	e, e	14.8
e, d	19.7	e, E	14.8
e, D	19.7		

effect of added proton donor	$\partial E_p/\partial(\log[HX])^b$ (mV/decade)[b]
if protonation occurs after the RDS	0
if protonation occurs before the RDS or is the RDS	same as $dE_p/d(\log v)^a$ but opposite sign

rate equation[d,e]	$\partial E_p/\partial(\log[A])$ (mV/decade)[b]	rate equation[d,e]	$\partial E_p/\partial(\log[A])$ (mV/decade)[b]
$k_{app}[B]$	0	$k_{app}[B]^2/[A]$	0
$k_{app}[A][B]$	29.6	$k_{app}[B]^2[A]$	39.4
$k_{app}[B]^2$	19.7		

[a] Parker, V. D. *Acta Chem. Scand.* **1980**, *34B*, 359. [b] At 25 °C; multiply by T (in °K)/298 to correct to a different temperature. [c] [HX] = concentration of added proton donor. [d] Rate equation as derived from the postulated mechanism. [e] [A] = concentration of electroactive substance; [B] = concentration of intermediate B.

(13) A full list of all 300 mechanistic possibilities is included with the supplementary material.

(14) Ahlberg and Parker have used these symbols in slightly different fashion: Ahlberg, E.; Parker, V. D. *Acta Chem. Scand.* **1980**, *34B*, 97.

(15) Parker, V. D. *Acta Chem. Scand.* **1980**, *34B*, 359.

for example, that a will be −29.6 mV/decade (at 25 °C)[16] for all mechanisms in which a single heterogeneous electron transfer precedes or is the rate-determining step (RDS) of the mechanistic sequence. Referring to Table 3, for example, mechanisms 5b, 5c, 17b, 17c, 10b, and 22b fall into this category. Mechanisms in which two heterogeneous electron transfers take place before or in the RDS ("e ... e" or "e ... E" type, e.g., mechanisms 5d, 10c, and 10d of Table 3) are predicted to exhibit a value of −14.8 mV/decade for a, and those in which the second electron transfer takes place in homogeneous solution before or in the RDS ("e ... d" or "e ... D" mechanisms, as in 17d, 22c, and 22d of Table 3) should exhibit a value of −19.7 mV/decade. Term b (*vide supra*) will be zero where cyclization is a simple first-order reaction; a nonzero value of b indicates a more complex cyclization mechanism.[2] Finally, c is zero if the protonation step occurs after the rate-determining step; otherwise, it is predicted to have the same absolute value as a. (Table 3 shows the predicted values of a, b, and c for several mechanistic families.) The values of the coefficients a, b, and c can be used in conjunction with chemical arguments and the results of preparative-scale electrolyses to reduce the larger list of mechanistic possibilities to a small list of reasonable candidates. Other electrochemical experiments may also shed useful light upon the reaction mechanism. If the rates of the coupled chemical reactions are not too high, they can be measured by a technique such as derivative cyclic voltammetry (DCV).[17] When this is possible, the full kinetic rate expression for one or more of the mechanisms under consideration may suggest further experiments, e.g., the effects of temperature, isotopic substitution, or added reagents (other than the proton donor) on the overall rate.[17]

Results

The example we selected for application of these ideas is the reductive cyclization of α,β-unsaturated esters bearing carbonyl groups in the ω-position to afford ω-hydroxy esters.[6] The substrate chosen for the voltammetric experiments is **6**, which has been shown to undergo reductive cyclization to **7** in good yield.[6]

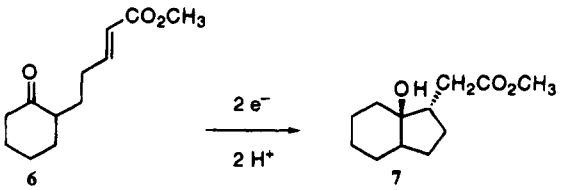

6 7

Voltammetry. LSV measurements were carried out at 21 °C relative to a Ag/0.1 M $AgNO_3$ reference electrode at a mercury-coated platinum electrode in dimethylformamide (DMF) containing tetrabutylammonium hexafluorophosphate (TBAHFP). DMF was rigorously dried (see Experimental Section) under conditions which have been shown to reduce its water content to under 1.5 ppm.[18] The electrolyte was also carefully dried and was employed at a concentration of 1.0 M in order to minimize errors due to uncompensated solution resistance, which, if significant, would have caused problems in interpretation of the LSV data. The concentration of **6** was also kept low in all experiments to keep faradaic currents low and therefore minimize iR errors.[19] Uncompensated iR errors were shown to be negligible by addition of azulene (0.5 mM) to the medium after the LSV experiments were complete and examination of its cyclic voltammetry (CV) behavior as a function of scan rate; the peak potentials were found to be independent of scan rate, as was the spacing between anodic and cathodic peak potentials. LSV measurements were carried out on **6** at a series of 12 concentrations over the range 5×10^{-5} to 10^{-3} M chosen such that their logarithms are approximately equally spaced. At each concentration, the peak potential was measured over a range of scan rates from 14 to 600 mV s^{-1}, also selected such that their logarithms are evenly spaced (some data were measured only up to 400 mV s^{-1}).

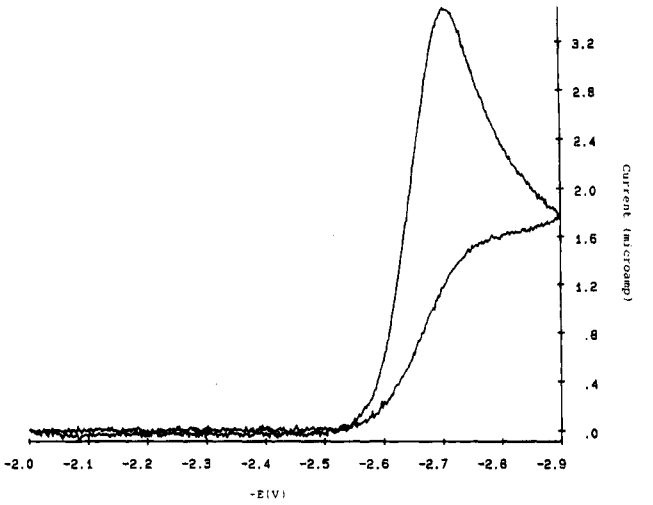

Figure 2. Cyclic voltammogram of **6** (1.02 mM) at 100 mV/s in dimethylformamide/1.0 M. tetrabutylammonium hexafluorophosphate with background subtracted.

E_p cannot be measured with accuracy directly from the experimental voltammograms because LSV peaks tend to be rather broad, but peak potentials can be measured with high accuracy from plots of di/dE vs E,[20] rather than from the usual plot of i vs E. We adopted this practice in the work described here. The signal-to-noise level in the linear sweep voltammograms was quite low at the lowest concentrations and one would therefore normally expect that the data would be unsatisfactory at these concentrations. However, it is easier to measure di/dE at low concentrations than it is to measure E_p because the background correction is smaller in the di/dE measurement (the background rises approximately linearly; hence, its derivative is approximately zero). We were able to obtain very reliable data even at the lowest concentrations employed. None of the voltammograms exhibited an anodic peak upon scan reversal after the cathodic peak, even at the fastest scan rates employed; a representative voltammogram is shown in Figure 2. The voltammetric peak potential data (recorded at 21 °C) are presented in Table 5.[21] Least squares analysis of the data in Table 5 provides average values for a and b of −29.0 and −2.9 mV/decade, respectively.

(16) These predicted slopes are multiples of $2.303RT/n\mathcal{F}$ and are therefore temperature dependent.[14]
(17) Parker, V. D. In *Topics in Organic Electrochemistry;* Fry, A. J., Britton, W. E., Eds.; Plenum: New York, 1986; Chapter 2.
(18) Burfield, D. R.; Smithers, R. H. *J. Org. Chem.*, **1978**, *43*: 3966.
(19) Parker, V. D. in Bard, A. J., ed., *Electroanalytical Chemistry;* Dekker: New York, 1986; Vol. 14, pp 1–111.
(20) Parker, V. D. *Acta Chem. Scand.* **1981**, *35B*, 373.
(21) LSV experiments require only small amounts of material; only 3.0 mg of **6** was required to obtain the data in Table 5.

Table 5. Linear Sweep Voltammetric Peak Potential ($-E_p$) for Keto Ester 6 as a Function of Concentration and Scan Rate[a]

	$-E_p$ for concentrations $\times 10^5$ M												
scan rate (mV/s)	4.38	6.13	8.36	13.09	17.54	26.12	34.70	43.30	53.95	60.53	81.59	102.49	b_v[b] (mV/decade)
14	2677.7	2699.5	2714.5	2689.4	2679.2	2674.3	2675.4	2681.9	2683.6	2679.2	2680.9	2695	−8.3
20	2680.0	2673.4		2679.6	2685.4	2675.9	2676	2678.3	2682.5	2676.6	2683.4	2684.5	+2.6
30	2686.1	2687.2	2700.4	2681.6	2679.9	2682.8	2683.1	2681	2685.6	2679.6	2683.6	2698.5	−1.5
40	2693.2	2694.7	2702.4	2696.8	2683.1	2684.8	2689.4	2686.4	2692.3	2680.9	2688.4	2692.2	−6.8
60	2699.5	2698.8	2699.6	2698.8	2688	2692.5	2692.2	2693.7	2696.8	2691.1	2693.6	2695.3	−4.5
80	2703.5	2706.3	2708.2	2698.9	2703.8	2694.6	2694.4	2693.9	2698.3	2692	2697.3	2699	−8.3
100	2704.7	2702.7	2711	2699.1	2694.1	2696.4	2696.8	2697.9	2700	2701.6	2698.6	2701.5	−4.2
125	2713.4	2713.0	2716.1	2708.3	2692.2	2699.1	2701.4	2701.8	2709.6	2701.9	2702.6	2706.2	−7.6
140	2705.1	2714.6	2716.2	2711	2694	2700.6	2704.3	2702.2	2707.9	2700	2704.2	2707.3	−5.4
200	2724.3	2723.2	2725.6	2714.6	2699.7	2711.5	2709	2713.2	2714.1	2705.7	2707.9	2714.5	−10.6
300	2718.1	2718.7	2724.7	2716.3	2716.5	2711.4	2713.6	2706.9	2720.4	2712.8	2716.3	2719.2	−3.5
400	2715.5	2733.5	2724.5	2719.4	2715.5	2714.9	2717.1	2719.5	2722.7	2714.8	2718.8	2722.8	−3.0
500					2719.5	2720.1	2721.4	2722.7	2725.9	2719.3	2722.9	2727.8	+8.3
600					2721.1	2720.9	2723.7	2726.7	2729.7	2721.4	2728.9	2730.1	+11.9
$-a_c$[c] (mV/decade)	31.3	31.8	26.4	27.0	26.7	29.8	30.5	29.7	30.6	29.3	29.4	25.6	

[a] $-E_p$, measured in 1.0 M Bu_4NPF_6 in dimethylformamide in millivolts vs Ag/0.1 M $AgNO_3$. [b] $b_v = \partial E_p/\partial(\log \text{concentration})$ at scan rate v. Average $b = -2.9$ mV/decade. [c] $a_C = \partial E_p/\partial(\log \text{scan rate})$ at concentration C. Average $a = -29.0$ mV/decade.

Table 6. Linear Sweep Voltammetric Peak Potentials ($-E_p$) for Keto Ester 6 as a Function of Phenol Concentration and Scan Rate[a]

	E_p for concentrations of 8 $\times 10^3$ M					
scan rate (mV/s)	0.77	1.15	1.53	2.27	3.00	c_v[b] (mV/decade)
20		2654	2662	2662	2636	36.7
30	2674	2650	2650	2654	2658	20.2
40	2678	2670	2670	2664	2654	36.5
60	2672	2666	2670	2664	2664	12.7
80	2692	2680	2674	2672	2676	27.8
100	2676	2672	2674	2666	2666	18.0
125	2686	2682	2668	2662	2676	27.8
140	2692	2688	2682	2674	2672	36.6
200	2696	2690	2698	2680	2678	31.8
300	2708	2692	2690	2686	2682	39.8
400	2698	2700	2692	2684	2676	40.0
500	2706	2696	2694	2694	2678	38.9
600	2704	2698	2700	2694	2690	35.4
$-a_c$[b] (mV/decade)	26.8	33.0	29.2	25.3	26.1	

[a] $-E_p$, measured on a 0.13 mM solution of **6** in 1.0 M Bu_4NPF_6 in dimethylformamide in mV vs Ag/0.1 M $AgNO_3$. [b] $a_c = \partial E_p/\partial(\log \text{scan rate})$ at phenol concentration C. Average $a = -28.1$. [c] $c_v = \partial E_p/\partial(\log \text{concentration of phenol})$ at scan rate v. Average $c = 31.2$ mV/decade.

Effect of Added Proton Donors. Since the cyclization reaction consumes two protons, it is important to know the response of the system to added proton donors. The effect of added 3,5-dimethylphenol (**8**)[22] was examined by adding the phenol in incremental amounts (Table 6).

The concentration of **6** and the initial concentration of **8** were chosen such that **8** was in excess in order to insure that protonation of intermediates followed pseudo-first-order kinetics. It was not possible to increase the concentration of **8** above 3 mM because of pronounced adsorption effects (erratic and irreproducible voltammetric behavior). Least-squares analysis of the data in Table 6 affords a value for $c \equiv \partial E_p/\partial \log[\mathbf{8}]$ of +31.2 mV/decade; a is −28.1 mV/decade for these data, as expected.[23]

(22) This phenol was chosen because it is less hygroscopic than phenol itself.

(23) A corresponding series of experiments involving addition of H_2O to a solution of **6** in rigorously dried DMF were carried out; the results are qualitatively similar to those involving added **8**, but the voltammograms were more noisy than when **8** was added, possibly because of the incursion of electroinitiated anionic polymerization or dianion precipitation.[2b]

Scheme 2

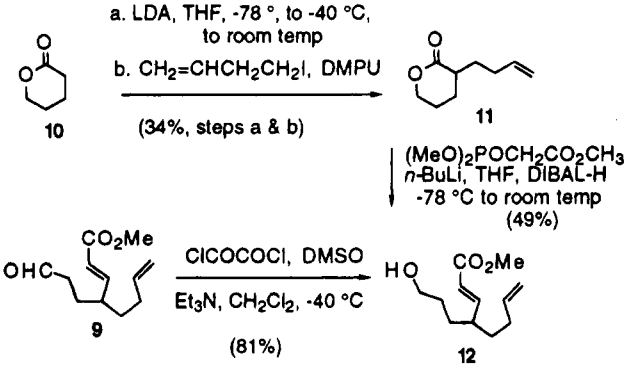

Synthesis and Electrochemical Reduction of a Test Substrate. It appeared that an appropriately designed substrate might permit us to make mechanistic distinctions not possible through electrochemical measurements alone. In particular, we realized that a substrate such as **9**, bearing carbonyl and vinyl groups in similar positions relative to the conjugated ester moiety, should provide information on the nature of the cyclizing intermediate (see Discussion). A straightforward synthesis of **9** is illustrated in Scheme 2. Of note is the use of the Takacs procedure[24] to convert lactone **11** to the unsaturated ester **12**. On several occasions, the R. D. Little laboratory has found this methodology to be superior to the alternative two-step protocol calling for reduction followed by the condensation reaction.

Controlled potential electrolysis of **9** was carried out in DMF/0.1 TBAHFP containing an excess of phenol **8**, i.e., under conditions designed to emulate the voltammetric experiments as closely as possible. The electrolysis produced 43% of hydroxy ester **13** and 38% of lactone **14** (isolated yields). Capillary column gas chromatographic analysis using biphenyl as an internal standard indicated a nearly quantitative yield of a 1:1 mixture of **13** and **14**. The latter is mechanistically equivalent to **13** and presumably arrives by cyclization of a late intermediate (anion **19**; see Discussion).

Discussion

As we have pointed out above, there are two families of mechanism available for the electroreductive cycliza-

(24) Takacs, J. M.; Helle, M. A.; Seely, F. L. *Tetrahedron Lett.* **1986**, *27*, 1257.

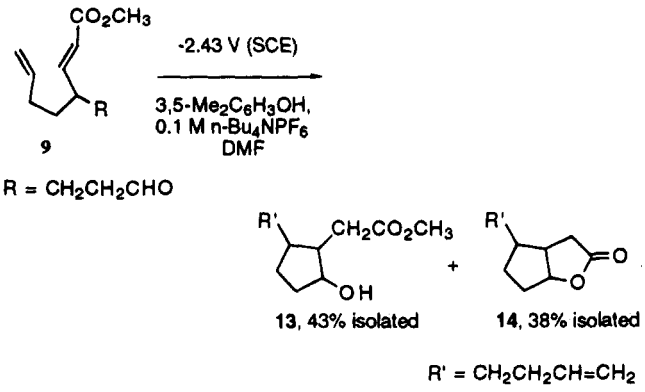

tion shown in Figure 1a, depending on whether A or B of **6** is the electroactive group... or electrophore. In the case of **6**, this ambiguity does not exist. α,β-Unsaturated esters are reduced at −2.3 to −2.5 V vs SCE,[25] whereas aliphatic aldehydes and ketones are difficult or impossible to reduce at all in dimethylformamide (DMF) or acetonitrile containing tetraalkylammonium salts as supporting electrolyte.[6,26] It is clear therefore that the electrophore in **6** is the α,β-unsaturated ester moiety.

We reduce the hypothetical 300 mechanisms possible for the hydrocyclization of **6** in the following way. (a) **6** contains no groups basic enough to be protonated to any significant extent by phenol. We may therefore exclude all mechanisms of Table 2 which are initiated by a protonation step (mechanisms 25−48) and also all mechanisms which imply protonation of neutral intermediates (mechanisms 6, 8, 9, 12, 18, 20, 21, and 24). (b) Likewise, the fact that α,β-unsaturated esters do not react spontaneously with ketones permits us to exclude all mechanisms in which the first step is a cyclization (mechanisms 49−60). (c) The observed value for *a* of −29.0 mV, close to the theoretical value of −29.2 mV (at −21 °C), demonstrates that a single electron-transfer step precedes or is the rate-determining step. (d) The value of *b* (−2.9 mV) is close to the theoretical value of 0 V; this demonstrates that the cyclization is kinetically first-order in **6**, i.e., that the cyclization is a simple unimolecular process.[27] (e) Mechanisms ending in a cyclization step (mechanisms 3, 11, 15, and 23 of Table 2) can be excluded because this implies that the saturated keto ester corresponding to **6** would spontaneously cyclize; this follows from the fact that the first four steps (two "e" and two "p" steps, in any order) would saturate the double bond of the α,β-unsaturated ester. (f) Finally, the experimental value of +31.2 mV for *c* permits us to conclude that a single proton transfer occurs before or in the rate-determining step.[14] This permits a final sharp reduction of the mechanistic possibilities to the following eight (these actually represent only four mechanisms, each in the form of an e...e and e...d pair, as discussed previously):

5c	e−c−P−e−p	17c	e−c−P−d−p}	radical anion closure
7b	e−P−c−e−p	19b	e−P−c−d−p }	radical closure
7c	e−p−C−e−p	19c	e−p−C−d−p}	
10b	e−P−e−c−p	22b	e−P−d−c−p}	anion closure

We assume that there are actually only four viable candidates, i.e., those in the second column, in which the second electron transfer is homogeneous.[12] Because the voltammetric results cannot distinguish among these possibilities, we require evidence from other sources to reduce this list further. At this point the results obtained in the electrolysis of compound **9** prove to be critically important. We note that mechanisms 5c, 10b, 17c, and 22b involve cyclization of anionic (carbanion or radical anion) intermediates, whereas in the other four mechanisms the cyclizing species is a free radical. As indicated in Table 7, intramolecular 5-*exo-trig* radical cyclizations onto vinyl and carbonyl π-bonds take place at similar rates.[28] However, the former process is irreversible, whereas the latter is reversible and indeed *thermodynamically disfavored*. Accordingly, the existence of a radical component to electroreductive cyclization should be expressed by isolation of products resulting from an irreversible cyclization onto the alkene. On the other hand, carbanions attack carbonyl groups much faster than alkenes, and addition is irreversible. One would therefore expect that cyclization ought to afford **15** if the cyclizing species is a radical, but **13** if it is a carbanion or radical anion.[29] In the event, as noted above, controlled potential electrolysis of **9** under conditions similar to those used for the voltammetry of **6** (2.5 mM in **9**, 25 mM in **8**) afforded *only* hydroxy ester **13** and lactone **14**, each resulting from *closure onto the carbonyl*. We were unable to detect the presence of radical-derived product **15** and conclude, therefore, that electroreductive cyclization does not proceed *via* radical cyclization involving either an e−P−c−d−p or an e−p−C−d−p pathway.

Table 7. Cyclization Rates of 5-Hexenyl Radicals

R	X	T (°C)	k_f (s^{-1})	k_{-f} (s^{-1})	ref
H	O	25	1.4×10^5	9.1×10^7	28a
CH_3	CH_2	25	2.9×10^{4a}	no back reaction	28b

[a] Rate for formation of the trans isomer. For the cis isomer, k_f $\sim 10^5$ s^{-1}.

Two paths remain, one involving cyclization of a radical anion (e−c−P−d−p), the other a carbanion (e−P−d−c−p). The former requires that the rate-determining step involve protonation of the "hard" oxyanion **16**, while the latter involves rate-determining protonation of the "soft" radical anion **17**. The rates of these two steps ought to differ despite the fact that each involves proton transfer. In particular, protonation of **16** by phenol **8** ought to occur rapidly given the *localized* nature of the anion, while protonation of **17** is expected to be slower because it is *delocalized*.[30] Arene radical anions (delocalized) indeed have been shown to be much less basic (thermodynamically) than structurally related carbanions.[31] Therefore, it appears unlikely that the protonation of **16** should correspond to the rate-determining step. Assuming this assessment is accurate, we are left to conclude that the electroreductive cyclization of **9** proceeds by the e−P−

(25) House, H. O.; Huber, L. E..; Umen, M. J. *J. Am. Chem. Soc.* **1972**, *94*, 8471.
(26) Fry, A. J. and Reed, R. G., unpublished experiments.
(27) It is typical to find somewhat larger errors in *b* than in *a*: Aalstad, B.; Ronlan, A.; Parker, V. D. *Acta Chem. Scand.* **1981**, *35B*, 247.
(28) (a) Beckwith, A. L. J.; Hay, B. P. *J. Am. Chem. Soc.* **1989**, *111*, 230. (b) Lusztyk, J.; Maillard, B.; Deycard, S.; Lindsay, D. A.; Ingold, K. U. *J. Org. Chem.* **1987**, *52*, 3509.
(29) Radical anions of activated alkenes react with electrophiles at the β-carbon: Degrand, C.; Mons, R.; Lund, H. *Acta Chem. Scand.* **1983**, *37B*, 429.
(30) (a) Kresge, A. J. *Acc. Chem. Res.* **1975**, *8*, 354; (b) Koch, H. F. *Acc. Chem. Res.* **1984**, *17*, 137.
(31) Parker, V. D; Tilset, M.; Hammerich, O. *J. Am. Chem. Soc.* **1987**, *109*, 7907.

Scheme 3

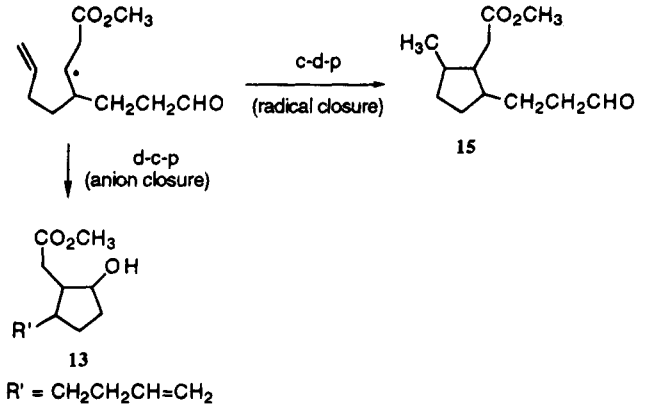

Scheme 4

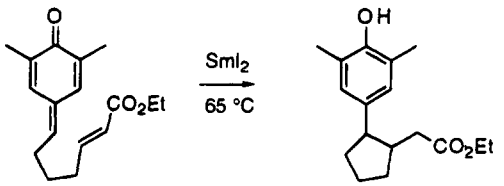

d–c–p path, involving *cyclization of an anion* (Scheme 3). (The closely related e–P–d–p pathway, also involving rate-determining protonation of a radical anion, has been observed previously).[32] Apparently, homogeneous electron transfer converting radical **18** to the corresponding carbanion **19** occurs faster than cyclization. The observation that ketone **20** fails to undergo cyclization, preferring instead to afford the product of saturation of the C–C π-bond,[6] is consistent with the proposed mechanism. We suggest that closure onto the *hindered* carbonyl carbon of **20** is slowed to the point where cyclization becomes the rate-determining step, thereby allowing the observed alternative path involving protonation of the anion to occur more rapidly.

It is important to note that the mechanistic conclusions we have reached here refer to the specific conditions under which our experiments were carried out, i.e., submillimolar concentrations of the electroactive substance and the scan rates used in the LSV experiments. The data in Table 6 naturally prompt the question of what the proton donor is in the absence of added phenol. We believe that the starting material is the proton source in the absence of added proton donor. Earlier work showed that yields in preparative experiments are low in the absence of added proton donors, probably because the electrogenerated anion of the starting material initiates a variety of base- and nucleophile-promoted reactions.[9] *At low conversion,* the reaction probably proceeds via the e–P–d–c–p path, either in the presence or absence of proton donor. There is, incidentally, no evidence that these experiments proceed by an electrocatalytic pathway. Interestingly, Lee *et al.* recently reported a study of the mechanism of reduction of substrates such as **6** by magnesium in methanol and concluded that the mechanism is (using our mechanistic terminology) e–P–e–c–p.[33] It is entirely possible that the mechanism of the latter reactions is actually e–P–d–c–p; the distinction could not have been made by their experiments.

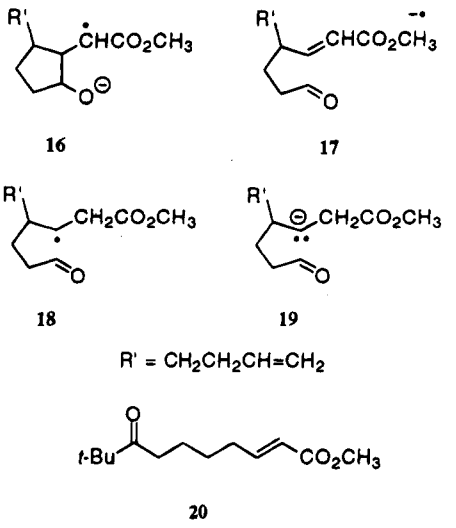

Further Implications. LSV is a powerful method for investigating reaction mechanisms and could be applied profitably to a number of non-electrochemical reductive or oxidative cyclizations in the literature whose mechanisms are unknown. [The reductive cyclization of quinone methides (Scheme 4) is in this category. It has been carried out by nonelectrochemical means,[34] but the nature of the cyclizing intermediate was unclear; presumably this question could by answered by an LSV investigation.]

However, as we developed Table 2, we realized that it could even be helpful in designing new electrochemical reactions. Most electrochemical cyclizations are initiated by electron transfer; their mechanisms will be found among those in columns 1 and 2 of Table 2. However, while certain types of mechanism will tend to be found relatively frequently, it is hard to say with certainty that any particular mechanism in Table 2 is *prima facie* unlikely. For example, it is not difficult to conceive of processes in which a chemical step initiates the electrocyclization sequence. Indeed, reductive cyclization of bisimines such as **4** does proceed by initial protonation, followed by reduction of the conjugate acid,[1c] but one could also conceive of processes in which addition or loss of a proton triggers cyclization followed by final oxidation or reduction, e.g., the hypothetical Nazarov rearrangement-*cum*-reduction illustrated in Scheme 5.[35] Hydrocyclizations initiated by cyclization (Table 3, columns 5 and 6) are likely to be uncommon, but one might imagine, for example, that they might be found in systems where an acyclic electroinactive species is in equilibrium with a minor, electroactive, cyclic isomer. The converse process, reduction or oxidation of the small amount of the open-chain isomer of glucose which is in equilibrium with its inactive cyclic hemiacetal form, has been known for many years.[36] Other examples might include electrocyclic ring opening of cyclobutenes followed by electrochemical reduction of the resulting 1,3-butadienes. Processes of this type, in which a chemical reaction unmasks an electroactive species, may require elevated temperatures to be observed. A category of electrohydrocyclization which might appear unlikely at first sight

(32) Nielsen, M. F.; Hammerich, O.; Parker, V. D. *Acta Chem. Scand.* **1986**, *B40*, 101.
(33) Lee, G. H.; Choi, E. B.; Lee, E.; Pak, C. S.; *J. Org. Chem.* **1994**, *59*, 1428.
(34) Angle, S. R.; Rainier, J. D. *J. Org. Chem.* **1992**, *57*, 6883.
(35) For references to the Nazarov rearrangement, see: Woodward, R. B.; Hoffmann, R. *The Conservation of Orbital Symmetry*, Verlag Chemie: Weinheim, 1971; p 58.
(36) (a) Wiesner, K. *Coll. Czech. Chem. Commun.* **1947**, *12*, 64. (b) Isbell, H. J.; Frush, H. L. *J. Res. Natl. Bur. Stand.* **1935**, *14*, 359.

Scheme 5

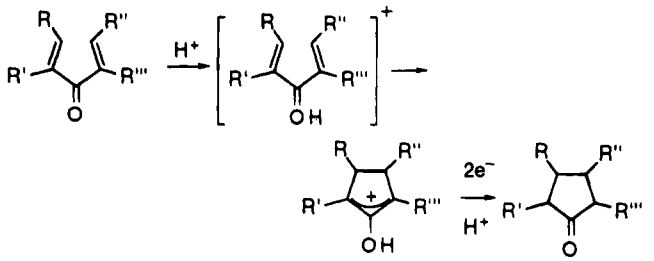

Scheme 6

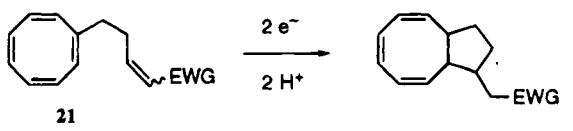

Scheme 7

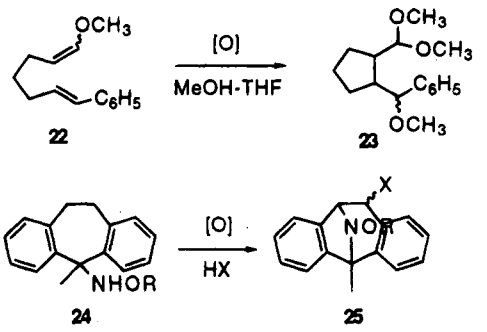

includes those reactions, e.g., mechanisms 3, 15, 33, and 45 of Table 2, in which cyclization occurs *after* transfer of two protons and two electrons. Generally, reactive intermediates cyclize, but one could imagine cases where the *product* of a redox process is prone to cyclization, perhaps because of orbital symmetry or ring strain considerations. A (non-electrochemical) example of such a process has in fact recently been reported by Nicolaou.[37] Processes in which the first step is of E type, i.e., in which the initial electron transfer is rate-determining, are found when the following chemical reactions are so fast that the initial charge transfer is not Nernstian, or where the initial electron transfer is quasi-reversible. The hypothetical cyclization of substituted cyclooctatetraene **21** shown in Scheme 6 might fall into this category, inasmuch as reduction of cyclooctatetraenes to their planar radical anions is quasi-reversible.[38] Unfortunately, LSV cannot afford mechanistic information about this type of process.

The procedure used here to determine the total number of possible mechanisms is of course not limited to intramolecular hydrocyclizations and dehydrocyclizations. It may be used for any redox process coupled to a chemical reaction, including ring-opening reactions, sigmatropic reactions, and cyclizations involving loss or addition of nucleophilic species other than protons, e.g., the anodic conversion of **22** to **23** or **24** to **25**[39] (Scheme 7). Mechanistic information in such cases may be obtained by measuring $\partial E_p/\partial \log[Nu]$.

(37) Nicolaou, K. C.; Liu, A.; Zeng, Z.; McComb, S. *J. Am. Chem. Soc.* **1992**, *114*, 9279.

(38) Fry, A. J. In *Topics in Organic Electrochemistry;* Fry, A. J., Britton, W. E., Eds.; Plenum: New York, 1986; p 12.

(39) (a) Karady, S.; Corley, E. G.; Abramson, N. L.; Weinstock, L. M. *Tetrahedron Lett.* **1989**, *30*, 2191. (b) Moeller, K. D.; Marzabadi, M. R.; New, D. G.; Chiang, M. Y.; Keith, S. *J. Am. Chem. Soc.* **1990**, *112*, 6123.

Experimental Section

General. Dimethylformamide was distilled at aspirator vacuum from CaH_2 and stored over 3-Å molecular sieve which had been activated at 300 °C overnight. After 3 days the DMF was transferred by cannula to a container equipped with a septum for withdrawal of solvent and containing freshly activated molecular sieve. This procedure has been shown to reduce the water content of DMF to <2 ppm.[18] Bu_4NPF_6 (TBAHFP) (Aldrich) was dried (Abderhalden) for 3 days at 100 °C. An older sample of compound **6**[6] which had been stored in a sealed ampoule was purified by flash chromatography; its NMR spectrum was identical with that of the original sample.

Evidence for compound purity was obtained using both ^1H and ^{13}C NMR spectroscopy. ^1H NMR spectra were recorded at 200, 300, or 500 MHz in $CDCl_3$, unless otherwise noted, and either Me_4Si or $CHCl_3$ (7.26 ppm) was used as the internal standard; all J values are in hertz. For ^{13}C NMR, $CDCl_3$ (77.0 ppm) was the internal standard. The abbreviation "dn" refers to a downward peak in the APT spectrum. For IR, the polystyrene peak at 1601 cm^{-1} was used as a reference. All reactions, unless otherwise noted, were carried out in oven- or flame-dried glassware under a N_2 atmosphere. Unless otherwise noted, solvents and reagents were purified by standard methods. Reactions and conditions are not optimized. Column chromatography refers to flash chromatography.

Voltammetry was carried out with the aid of a Cypress Systems Model CS 1090 computer-driven electrochemical data acquisition system, using the Cypress version 6.01 software to generate waveforms and acquire data. Strictly speaking, the experiment being carrried out is staircase voltammetry (SCV), not LSV, but voltammetric currents were measured at times corresponding to 0.25 of the step time; under these conditions SCV and LSV peak potentials are very similar.[40] A Brinkmann Instruments voltammetry cell #EA875-20 was used and the cell utilities were contained in standard 14/20 adapters for ease and reproducibility of cell assembly. The cathode was a platinum disk coated with mercury in the following manner. An 0.5-mm platinum wire was sealed into soft glass tubing and the end was ground off to expose the end of the wire. A small amount of solder was placed inside the tubing and melted, and a platinum wire was immersed in the molten solder before it cooled, to provide electrical contact to the electrode. Platinum black was plated onto the cathode, which was then coated with mercury by dipping.[41] The construction of the $Ag/AgNO_3$ reference electrode has been described previously.[42] Solutions were degassed by bubbling argon through the solution for 30 min at the outset and again after addition of any substance to the cell. A standard taper adapter equipped with a large serum cap was installed in one of the cell ports, and two needles (for argon introduction and escape) were inserted through the serum cap. The counter-electrode was a platinum wire. Voltammograms were measured on 1.0 M solutions of TBAHFP in order to minimize uncompensated iR errors, although it is likely that salt concentrations as low as 0.5 M would have sufficed for this purpose.[43] After background subtraction, the digitized voltammograms were ported to a commercial plotting program[44] for differentiation and smoothing. E_p, which by definition is the point at which the di/dE plot crosses the potential axis, was determined by interpolation between the two data points flanking the crossing point. The data in Tables 5 and 6 were inserted into spreadsheets (Excel) for computation of a, b, and c.

4-Iodo-1-butene. Commercially available 4-bromo-1-butene (6.77 g, 59.3 mmol) was placed into a round bottom flask

(40) Bilewicz, R.; Osteryoung, R. A.; Osteryoung, J. *Anal. Chem.* **1986**, *58*, 2761.

(41) (a) Van der Leest, R. *Anal. Chim. Acta* **1970**, *52*, 151; (b) Ramaley, L.; Brubaker, R. L.; Enke, C. G. *Anal. Chem.* **1963**, *35*, 1088; (c) Marrese, C. A. *Anal. Chem.* **1987**, *59*, 217.

(42) Fry, A. J.; Touster, J. *J. Org. Chem.* **1986**, *51*, 3905.

(43) Kadish, K. M.; Ding, J. Q.; Malinski, T. *Anal. Chem.* **1984**, *56*, 1741.

(44) Hyperplot (JHM International, Columbus, OH 43214).

containing 89 mL of reagent grade acetone and NaI (13.4 g, 89.1 mmol) and refluxed for 23 h. To this reaction was added 150 mL of Et_2O and then it was extracted with brine (3 × 150 mL). The organic layer was dried over $MgSO_4$, and the organic volatiles were distilled up to 60 °C (atmospheric pressure). The crude organic was transferred with minimal Et_2O and pentane to a smaller round bottom flask, and the volatiles were distilled to 80 °C (atmospheric pressure). The remaining oil was distilled to give a slightly pink liquid, bp 59 °C/69 Torr (6.63 g, 61%), whose structure was confirmed by comparison to literature ^1H and ^{13}C NMR spectral data.[45]

2-(3-Butenyl)-5-hydroxypentanoic Acid Lactone (11). In a procedure similar to that described by Schlessinger,[46] commercially available δ-valerolactone (**10**) (3.38 g, 33.8 mmol) was added via cannula to a −78 °C solution of LDA (33.8 mmol) in 34 mL of THF and 17 mL of *N,N'*-dimethylpropyleneurea (DMPU) over a 20 min. period. After an additional 20 min 4-iodo-1-butene (6.76 g, 37.2 mmol) was added followed by DMPU (13 mL). This solution was warmed to −40 °C and allowed to warm slowly to room temperature overnight. The reaction was poured into a separatory funnel along with Et_2O (200 mL) and brine (100 mL). The aq layer was extracted with Et_2O (7 × 100 mL). The organic layers were combined, dried over Na_2SO_4, and concentrated *in vacuo* to give an oil (16.44 g) which was chromatographed on silica with 1:1 Et_2O:pentane. The appropriate fractions from this column were then further purified by using a silica column with 35% Et_2O/65% pentane as the solvent to give pure **11** (1.76 g, 34%): TLC 40% Et_2O/60% pentane, I_2 stain, R_f (**11**) 0.20; ^1H NMR (200 MHz, $CDCl_3$) δ 5.92−5.67 (m, 1H), 5.13−4.92 (m, 2H), 4.29 (t, J = 5.71, 2H), 2.58−2.38 (m, 1H), 2.26−1.98 (m, 4H), 1.98−1.80 (m, 2H), 1.61−1.41 (m, 2H); ^{13}C NMR (75 MHz, $CDCl_3$) (APT assignment) δ 174.0 (up), 137.2 (dn), 114.6 (up), 67.6 (up), 37.9 (dn), 30.2 (up), 29.6 (up), 23.8 (up), 21.4 (up); IR (neat/NaCl) ν max (intensity) 3081 (m, sp^2 CH), 1741 (s, C=O), 1644 (m, C=C), 1260 (m, C−O), 1160 (m, C−O); LRMS (EI), *m/z* (relative intensity) 154.2 (M^+); exact mass [HRMS (EI)] calcd for $C_9H_{14}O_2$ 154.0994, found 154.0991.

Methyl 2(*E*)-4-(3-Butenyl)-7-hydroxyheptenoate (12). Compound **12** was prepared by adapting a procedure developed by Takacs.[24] To a −78 °C solution of trimethyl phosphonoacetate (327 mg, 1.79 mmol) in 10 mL of THF was added 1.2 mL (1.80 mmol) of 1.5 M *n*-BuLi in hexanes. After stirring for 45 min, **11** (250 mg, 1.62 mmol) in 1 mL of THF at −78 °C was added via cannula. After 30 min, 1.62 mL (1.62 mmol) of room temperature 1 M DIBAL-H in hexanes was added over a 20-min period. This solution was allowed to stir at −78 °C for 3 h and then warmed to rt over 13 h. To the hazy solution was added sodium potassium tartrate tetrahydrate (0.96 g, 3.40 mmol) in 6.8 mL of water (0.5 M). After 30 min of vigorous stirring, another 2 mL of water was added. After an additional 60 min of stirring, the clear organic layer and hazy aq layer were poured into a separatory funnel along with 15 mL of Et_2O and 15 mL of H_2O. The aq layer was drained off and the organic layer was washed with H_2O (1 × 20 mL) and then brine (1 × 20 mL). The organic layer was dried over $MgSO_4$ and concentrated *in vacuo* to give a light yellow oil (327 mg). The oil was chromatographed by a 3 × 27 cm silica column using 40% Et_2O/60% pentane as the solvent to give **12** (169 mg, 49%): ^1H NMR (200 MHz, $CDCl_3$) δ 6.69 (dd, J = 15.7, 15.7, 1H), 5.87−5.56 (m, 1H), 5.77 (d, J = 15.7, 1H), 5.06−4.82 (m, 2H), 3.69 (s, 3H), 3.61−3.46 (m, 2H), 2.28−2.07 (m, 1H), 2.07−1.82 (m, 3H), 1.64−1.26 (m, 6H); ^{13}C NMR (75 MHz, $CDCl_3$) (APT) δ 166.0 (up), 153.0 (dn), 138.0 (dn), 121.2 (dn), 114.8 (up), 62.5 (up), 51.4 (dn), 41.8 (dn), 32.4 (up), 31.2 (up), 30.4 (up), 30.2 (up); IR (neat/NaCl) ν max (intensity) 3410 (bm, OH), 3075 (w, sp^2 CH), 1730 (s, C=O), 1215 (m, C−O) cm^{-1}; LRMS (CI, CH_4), *m/z* 213 (MH^+); exact mass [HRMS, EI] calcd for $C_{11}H_{17}O_2$ ($M-CH_3O$) 181.1229, found 181.1253.

Methyl 2(E)-4-(3-Butenyl)-7-oxoheptenoate (9). To a stirred solution of DMSO (0.10 mL, 1.41 mmol) in CH_2Cl_2 (2 mL) at −40 °C was added 0.26 mL of a 2.0 M solution of oxalyl chloride (0.52 mmol) in CH_2Cl_2. After 20 min, **12** (79 mg, 0.37 mmol) in CH_2Cl_2 (0.5 mL) at −40 °C was added via cannula to the clear solution at which point the reaction mixture turned white. After 25 min, Et_3N (0.57 mL, 4.1 mmol) was added, causing the mixture to turn even whiter. After 30 min at -40 °C, the reaction mixture was allowed to stir another 35 min at rt. The reaction was quenched using 2 mL of H_2O; H_2O (10 mL) and CH_2Cl_2 (10 mL) were then placed in a separatory funnel along with the reaction mixture; the lower organic layer was removed. The aq layer was then washed with CH_2Cl_2 (3 × 12 mL). The organic layers were combined, washed with brine, dried over $MgSO_4$, and concentrated *in vacuo* to give a mixture of **9** and some Et_3N·HCl. To remove Et_3N·HCl and baseline impurities, the mixture was passed through a 1 × 17 cm silica gel column with 50:50 Et_2O/pentane and a single 250-mL fraction was collected. This was then concentrated and the remaining oil was purified by a 1 × 27 cm silica gel column with 20% Et_2O/80% pentane as the solvent to give **9** (64 mg, 81%) as a colorless oil: TLC 60%Et_2O/40% pentane, I_2 stain, R_f (**9**) 0.53; ^1H NMR (200 MHz, $CDCl_3$) δ 9.73 (t, J = 1.4, 1H), 6.64 (dd, J = 15.7, 15.6, 1H), 5.80−5.61 (m, 1H), 5.78 (d, J = 15.7, 1H), 5.06−4.88 (m, 2H), 3.71 (s, 3H), 2.40 (tt, J = 8, 2, 2H), 2.32−2.08 (m, 1H), 2.08−1.90 (m, 2H), 1.89−1.70 (m, 1H), 1.69−1.30 (m, 3H); ^{13}C NMR (50 MHz, $CDCl_3$) (APT) δ 201.6 (dn), 166.6 (up), 151.7 (dn), 137.7 (dn), 122.0 (dn), 115.1 (up), 51.5 (dn), 41.5 (up), 41.3 (dn), 33.4 (up), 31.1 (up), 26.3 (up); IR (neat/NaCl) ν max (intensity) 3070 (w, sp^2 CH), 2825 (w), 2715 (w, RCHO), 1730 (bs), 1660 (m, C=C), 1645 (m, C=C) cm^{-1}; LRMS (EI), *m/z* (relative intensity) 193.5 ([M + H - H_2O]$^+$, 4.8), 179.5 ([M + H − MeOH]$^+$); exact mass [HRMS, CI, CH_4] calcd for $C_{12}H_{19}O_3$ (M + H) 211.1334, found 211.1333.

Preparative Electrolysis of 9. A 0.1 M solution of *n*-Bu_4NPF_6 in DMF (100 mL) under Ar was placed in the anodic chamber of an H-cell. A Pt electrode was used as the anode. In the cathodic chamber was placed a 0.1 M solution of *n*-Bu_4NPF_6 and 3,5-dimethylphenol (338 mg, 2.77 mmol) in DMF (83 mL) along with a Hg cathode and an SCE reference electrode. (These different volumes were needed to obtain equal solution heights in the cell.) Compound **9** (58.1 mg, 0.277 mmol) was added and the solution was electrolyzed at −2.43 V vs SCE.

After the passage of 53.4 C, the catholyte was poured into a separatory funnel along with Et_2O (200 mL) and H_2O (200 mL). The layers were separated, and the organic layer was extracted with H_2O (2 × 100 mL). Solid NaCl was added to the combined aq layers, and they were extracted with Et_2O (3 × 150 mL). The organic layers were combined and passed through Celite to remove insoluble *n*-Bu_4NPF_6. The solution was dried over $MgSO_4$, passed through a 4 × 9 cm silica plug, and concentrated.

Gas chromatographic analyses were carried out on a Hewlett-Packard model 5890 gas chromatograph (GLC) equipped with a 60-m J&W 5% phenylmethylpolysiloxane capillary column using biphenyl as internal standard. Response factors for **9**, **13**, and **14** were 1.90, 2.22, 2.66, respectively. By GLC, this reaction gave approximately a 1:1 mixture of **13** and **14** in quantitative yield.

To remove the 3,5-dimethylphenol, the oil was dissolved in Et_2O (100 mL) and extracted with 5% aq NaOH (3 × 100 mL), satd aq $NaHCO_3$ (1 × 50 mL), and brine (1 × 50 mL). The solution was dried over $MgSO_4$ and concentrated *in vacuo* to give a yellow solid (108 mg) which was chromatographed on silica with CH_2Cl_2 (750 mL), followed by 95% CH_2Cl_2/5% Et_2O (1 L) to give hydroxy ester **13** (23.5 mg, 43%) and a mixture of lactone **14** (17.9 mg, 38%) and recovered starting material **9** (3.7 mg).

Spectral data for compound **13**: ^1H NMR (500 MHz, $CDCl_3$) δ 5.84 −5.74 (m, 1H), 5.04−4.92 (m, 2H), 3.92 (q, J = 6.5,1H), 3.70 (s, 3H), 3.13 (bs, 1H), 2.61 (dd, J = 16.5,4.0, 1H), 2.28 (dd, J = 16.5, 10.5, 1H), 2.20−2.05 (m, 1H), 2.05−1.85 (m,-2H), 1.85−1.75 (m,1H), 1:75−1.53 (m, 4H), 1.53−1.35 (m, 1H), 1.35−1.23 (m, 2H); ^{13}C NMR (50 MHz, $CDCl_3$) (APT) δ 175.1 (up), 138.6 (dn), 114.5 (up), 79.1 (dn), 51.9 (dn), 50.5 (dn), 43.6 (dn), 37.3 (up), 33.8 (up), 32.8 (up), 32.1 (up), 28.7 (up); FTIR (neat/NaCl) ν max (intensity) 3440 (bs, OH), 3076 (w, sp^2 CH),

(45) (a) Samsel, E. G.; Kochi, J. K. *J. Am. Chem. Soc.* **1986**, *108*, 4790. (b) Schurink, H. B. In *Organic Syntheses;* Blatt, A. H., Ed.; Wiley: New York, 1943; Collect. Vol. II, p 477.

(46) Herrmann, J. L.; Schlessinger, R. *J. Chem. Soc. Chem. Commun.* **1973**, 711.

1734 (s, ester C=O), 1639 (w, C=C), 1171 (m, C–O) cm^{-1}; LRMS (EI) m/z 212 (M^+), 152, 139, 134, 121, 108, 93, 87, 83, 79, 74, 67, 59, 55, 51, 43; exact mass [HRMS, EI] calcd for $C_{12}H_{18}O_2$ (M – H_2O) 194.1307, found 194.1316.

Spectral data for compound **14**: ^1H NMR (500 MHz, $CDCl_3$) δ 5.85–5.73 (m, 1H), 5.07–4.92 (m, 3H), 2.77 (dd, J = 18.5, 10.0, 1H), 2.40–2.31 (m, 1H), 2.18–1.84 (m, 6H), 1.78–1.67 (m, 1H), 1.57–1.47 (m, 1H), 1.42–1.21 (m, 2H); ^{13}C NMR (125 MHz, $CDCl_3$) δ 177.32, 138.08, 114.82, 86.22, 45.72, 45.26, 35.11, 33.68, 32.25, 31.91, 30.50; FTIR (neat/NaCl) v max (intensity) 3076 (w, sp^2 CH), 1772 (s, C=O), 1762 (m, C=O), 1639 (w, C=C), 1167 (m, C–O) cm^{-1}; LRMS (EI), m/z 139 (M – C_3H_5); exact mass [HRMS, EI] calcd for $C_8H_{11}O_2$ (M - C_3H_5) 139.0759, found 139.0749.

Acknowledgment. Financial support by the National Science Foundation and the Electric Power Research Institute is gratefully acknowledged: AJF (CHE-9100943); RDL (EPRI/NSF CHE-9208672).

Supplementary Material Available: A listing of the 300 possible electrocyclization/dehydrocyclization mechanisms and spectral data for compounds **9** [IR, LRMS, HRMS, ^1H NMR (200 MHz), ^{13}C APT, COSY, HETCOR, CV (with and without proton donor)] **11** [IR, LRMS, HRMS,^1H NMR (200 MHz), ^{13}C APT, HETCOR], **12** [IR, LRMS, HRMS, ^1H NMR (200 MHz), ^{13}C APT], **13** [FTIR, LRMS, HRMS, ^1H NMR (500 MHz), ^{13}C NMR, ^{13}C APT, COSY], and **14** [FTIR, LRMS, HRMS, ^1H NMR (500 MHz), ^{13}C NMR] (21 pages). This material is contained in libraries on microfiche, immediately follows this article in the microfilm version of the journal, and can be ordered from the ACS; see any current masthead page for ordering information.